HHS Public Access

Author manuscript

*Biol Psychiatry*. Author manuscript; available in PMC 2017 October 01.

Published in final edited form as:

*Biol Psychiatry*. 2016 October 01; 80(7): 522–533. doi:10.1016/j.biopsych.2016.04.023.

# Increased Metabotropic Glutamate Receptor 5 Signaling Underlies Obsessive-Compulsive Disorder-like Behavioral and Striatal Circuit Abnormalities in Mice

**Kristen K. Ade**, **Yehong Wan**, **Harold C. Hamann**, **Justin K. O'Hare**, **Weirui Guo**, **Anna Quian**, **Sunil Kumar**, **Srishti Bhagat**, **Ramona M. Rodriguiz**, **William C. Wetsel**, **P. Jeffrey Conn**, **Kafui Dzirasa**, **Kimberly M. Huber**, and **Nicole Calakos**

Departments of Neurology (KKA, YW, HCH, JKO'H, AQ, SB, NC), Neurobiology (KKA, YW, HCH, JKO'H, SB, NC), and Psychiatry and Behavioral Sciences (SK, RMR, WCW, KD), Duke University Medical Center, Durham, North Carolina; Department of Neuroscience (WG, KMH), University of Texas Southwestern Medical Center, Dallas, Texas; and Department of Pharmacology (PJC), Vanderbilt University Medical Center, Nashville, Tennessee.

## Abstract

**BACKGROUND—**Development of treatments for obsessive-compulsive disorder (OCD) is hampered by a lack of mechanistic understanding about this prevalent neuropsychiatric condition. Although circuit changes such as elevated frontostriatal activity are linked to OCD, the underlying molecular signaling that drives OCD-related behaviors remains largely unknown. Here, we examine the significance of type 5 metabotropic glutamate receptors (mGluR5s) for behavioral and circuit abnormalities relevant to OCD.

**METHODS—***Sapap3* knockout (KO) mice treated acutely with an mGluR5 antagonist were evaluated for OCD-relevant phenotypes of self-grooming, anxiety-like behaviors, and increased striatal activity. The role of mGluR5 in the striatal circuit abnormalities of *Sapap3* KO mice was further explored using two-photon calcium imaging to monitor striatal output from the direct and indirect pathways. A contribution of constitutive signaling to increased striatal mGluR5 activity in *Sapap3* KO mice was investigated using pharmacologic and biochemical approaches. Finally, sufficiency of mGluR5 to drive OCD-like behavior in wild-type mice was tested by potentiating mGluR5 with a positive allosteric modulator.

**RESULTS—**Excessive mGluR5 signaling underlies OCD-like behaviors and striatal circuit abnormalities in *Sapap3* KO mice. Accordingly, enhancing mGluR5 activity acutely recapitulates these behavioral phenotypes in wild-type mice. In *Sapap3* KO mice, elevated mGluR5 signaling is associated with constitutively active receptors and increased and imbalanced striatal output that is acutely corrected by antagonizing striatal mGluR5.

Address correspondence to Nicole Calakos, M.D., Ph.D., Duke University Medical Center, Neurobiology and Neurology, Box 2900, BRB Rm 201E - Neurology, Durham, NC, 27710; nicole.calakos@duke.edu.

**DISCLOSURES**

All authors report no biomedical financial interests or potential conflicts of interest.

Supplementary material cited in this article is available online at http://dx.doi.org/10.1016/j.biopsych.2016.04.023

**CONCLUSIONS—**These findings demonstrate a causal role for increased mGluR5 signaling in driving striatal output abnormalities and behaviors with relevance to OCD and show the tractability of acute mGluR5 inhibition to remedy circuit and behavioral abnormalities.

## Keywords

Circuit; Constitutive activity; mGluR5; Obsessive-compulsive disorder; Positive allosteric modulator; Striatum

Obsessive-compulsive disorder (OCD) is a debilitating neuropsychiatric disorder affecting 1%–3% of the population worldwide (1,2). Numerous studies in both patient populations and mouse models indicate that corticostriatothalamocortical circuit dysfunction, particularly increased activity in the striatum (3–7), drives the behavioral manifestations of OCD. However, the molecular mechanisms underlying this disorder remain largely unknown.

Mice with genetic deletion of *Sapap3* (a postsynaptic scaffold protein gene, also known as DLGAP3/GKAP3) provide a relatively unique opportunity to study the molecular mechanisms underlying OCD-relevant behaviors. *Sapap3* knockout (KO) mice demonstrate several OCD-like phenotypes, including increased striatal activity (4), increased anxiety-like behaviors (8), and excessive and pathologic self-grooming that persists despite causing harmful facial lesions (8). OCD-like behaviors in *Sapap3* KO mice are treated by chronic fluoxetine (8), a first-line treatment for OCD, and several human genetic studies provide additional, although modest, support for construct validity (9–11). Finally, selective restoration of *Sapap3* expression in the striatum prevents the self-grooming and anxiety phenotypes of *Sapap3* KO mice (8), a finding that connects brain regions implicated by human studies (5–7) to the expression of OCD-like behaviors in this mouse model.

Previously, we demonstrated that a number of excitatory synaptic abnormalities in the dorsolateral striatum of *Sapap3* KO mice arise from overactive type 5 metabotropic glutamate receptor (mGluR5) signaling (12,13), leading us to hypothesize that excessive mGluR5 signaling drives OCD-like behavioral and circuit phenotypes. Indeed, mGluR5 antagonists are efficacious in reducing anxiety-like and repetitive behaviors in mouse models (14–16). However, the diversity of signaling pathways targeted by drugs with demonstrated efficacy [e.g., selective serotonin reuptake inhibitors (3,8), *N*-methyl-D-aspartate–type glutamate receptor antagonists (17), mGluR4 positive allosteric modulators (18), benzodiazepines and gamma-aminobutyric acid type A receptor agonists (19), as well as a number of treatments with unspecified or atypical mechanisms of action (20–22)] highlights the complexity of inferring molecular mechanism from treatment response, especially when the mechanism of the behavioral mouse model itself is unknown (14,15). In this study, we sought to establish whether increased mGluR5 signaling plays a causal role in driving OCD-relevant phenotypes.

# METHODS AND MATERIALS

## Animals

All animal procedures were performed in accordance with protocols approved by the Institutional Animal Care and Use Committee of Duke University. Generation of *Sapap3* KO, *Grm5* KO, and line 6 *Drd1a*-tdTomato transgenic mice has been previously described (8,23,24).

## Behavioral Experiments

Repetitive self-grooming and anxiety-like behaviors were assessed using open field (OF), light-dark emergence (LDE), and elevated zero maze (EZM) tests using methods previously described (25,26) (Supplement).

## In Vivo Recordings

Mice were surgically implanted with microarray recording electrodes using previously described methods (27). Briefly, 32 electrodes were implanted bilaterally into the dorsal striatum. After a recovery period (minimum of 3 weeks), neurophysiologic recordings were performed in an empty cage similar to the home cage. Complete details are available in the Supplement.

## Slice Electrophysiology

Acute coronal brain slices (300 μm) were obtained for electrophysiologic recordings as previously described (13). *Drd1a*-tdTomato transgene expression was used to distinguish between striatal projections belonging to the direct (fluorescent) and indirect (nonfluorescent) pathways (23). Whole-cell patch-clamp recordings obtained at 23°C–25°C were used to measure excitatory postsynaptic currents using methods described in the Supplement.

## Calcium Imaging

Slices were prepared, and calcium imaging experiments were performed and analyzed as described in O'Hare *et al.* (28). Briefly, acute parasagittal (300 μm) slices, corresponding to tissue approximately 300–900 μm medial to the first visible lateral aspect of dorsal striatum, were bulk loaded with the calcium indicator dye, Fura-2 AM (F-1221; Thermo Fisher Scientific, Waltham, MA) (Supplement).

Slices were transferred to the microscope chamber and continuously perfused with imaging solution containing (in mmol/L) 124 NaCl, 4.5 KCl, 1.2 $NaH_2PO_4$, 4 $CaCl_2$, 1 $MgCl_2$, 26 $NaHCO_3$, and 10 $_D$-glucose. Fluorescence images were acquired using a Ti:Sapphire laser (Chameleon Ultra I; Coherent) and Prairie View image acquisition software (Bruker Corp., Billerica, MA). To monitor action potentials (APs) with single-cell resolution, we performed vector line-scan imaging of the Fura-2 signal excited by 770 nm light. A concentric bipolar stimulating electrode (FHC, Inc., Bowdoin, ME) was placed on the cortical edge of the corpus callosum (Figure 2A), and slices were subjected to a series of extracellular stimuli ranging from subthreshold to suprathreshold intensities delivered in 10 single square pulses at 0.05 Hz. For additional image acquisition and analysis details, see the Supplement.

### Co-immunoprecipitation and Western Blotting

Striata were dissected from wild-type (WT) and *Sapap3* KO mice and quickly frozen over dry ice. Tissue was solubilized in co-immunoprecipitation buffer (50 mmol/L Tris, pH 7.4, 120 mmol/L NaCl, 1% Triton X-100), and the soluble lysate (200 μg of protein) was tumbled overnight at 4°C with 1 mg of anti-Homer antibody (D-3 sc-17842; Santa Cruz Biotechnology, Dallas, TX), which recognizes the long but not the short Homer 1a isoform (KM Huber, Ph.D., unpublished observations, June 2011) or mouse immunoglobulin G (sc-2025; Santa Cruz Biotechnology). Protein A/G agarose bead slurry (No. 20421; Thermo Scientific) was added for 1 additional hour, and the beads were washed with co-immunoprecipitation buffer. Western blotting was performed using primary polyclonal antibodies that recognize either mGluR5 (AB5675; Millipore, Temecula, CA) or Homer (E-18 sc-8921; Santa Cruz Biotechnology).

### Statistical Analysis

Two-way repeated-measures analysis of variance and unpaired *t* tests were used to determine statistical significance for behaviors in the OF, LDE, and EZM. Values outside three standard deviations were considered outliers and were excluded from analysis [one value for KO vehicle and two values for KO 3-((2-methyl-1,3-thiazol-4-yl)ethynyl)pyridine hydrochloride (MTEP) in the LDE test]. The effects of drug and vehicle on the in vivo striatal neuron firing rates were determined using one-sample and unpaired *t* tests. Unpaired Student *t* tests were used to evaluate drug effects on miniature excitatory postsynaptic currents (mEPSCs). Two-way analysis of variance was used to compare conditions for input-output experiments. Unpaired Student *t* tests were used to determine statistical significance for the Western blot experiments.

## RESULTS

### mGluR5 Antagonism Reduces OCD-like Phenotypes of *Sapap3* KO Mice

To determine the significance of mGluR5 signaling for the expression of OCD-relevant phenotypes, we first evaluated the effects of the short-acting mGluR5 negative allosteric modulator (NAM), MTEP, on the increased self-grooming and anxiety-like behaviors of *Sapap3* KO mice. As previously reported (8), *Sapap3* KO mice spent significantly more time grooming in the OF than WT control mice (WT: 10.7% 6 0.2%, $n = 23$; KO: 23.2% ± 1.5%, $n = 24$; $F_{1,45} = 6.9$, $p = .01$). A single intraperitoneal (i.p.) injection of MTEP rapidly reduced elevated *Sapap3* KO grooming activity ($F_{1,22} = 6.7$; $p = .02$) but did not significantly modify basal grooming behavior of WT control mice, although there was a nonsignificant trend toward increased grooming after injection in the vehicle-treated cohort (Figure 1A, B).

In addition, consistent with prior observations (8), *Sapap3* KO mice spent significantly less time in the center of the OF during the baseline period compared with WT littermates (WT: 61.4% ± 0.6%; KO: 44.8% ± 1.6%; $F_{1,45} = 8.3$, $p = .006$), indicating an anxiety-like phenotype. MTEP treatment corrected this *Sapap3* KO phenotype (Figure 1C, D), although in this case the effect was more transient than the grooming response (paired *t* test for minutes: 210 to 0 and 10–20; $t_{11} = 2.6$, $p = .03$). MTEP did not significantly affect center

time in WT mice. MTEP treatment did increase locomotion in the OF, although this effect was transient and observed in both genotypes (Figure 1E).

We further investigated the anxiolytic effects of MTEP using the EZM and LDE tests. Compared with *Sapap3* KO mice treated with vehicle, MTEP-treated *Sapap3* KO mice spent more time in the open arms of the EZM and emerged to the brightly lit chamber of the LDE with shorter latencies (Figure 1F, H). MTEP treatment had no significant effects on any measure of anxiety in WT mice (Supplemental Figure S1). These experiments demonstrate that mGluR5 activity contributes to the heightened anxiety-like phenotypes of *Sapap3* KO mice.

We next examined whether mGluR5 signaling contributes to the elevated striatal activity of *Sapap3* KO mice (4), a circuit property that correlates with OCD symptoms in both patients (5–7) and mouse models (3,4). We performed in vivo recordings of neurons in the dorsal striatum using multielectrode arrays (27) and evaluated how firing rates of striatal units in *Sapap3* KO mice changed after i.p. injections of either vehicle or MTEP. Mice were exposed to either vehicle or drug on alternating consecutive days. Whereas vehicle injections had no significant effect, MTEP treatment significantly reduced striatal activity in *Sapap3* KO mice (Figure 1K, L). Similar treatment of WT control mice also showed a statistically significant reduction (Supplemental Figure S1F); however, consistent with excessive mGluR5 signaling in the OCD model mice, *Sapap3* KO mice showed a nearly twofold greater effect (Supplemental Figure S1G).

### Striatal mGluR5 Signaling Increases and Unbalances Striatal Output

Given the robust effects of systemic mGluR5 NAM treatment for reducing striatal firing in vivo (Figure 1K, L) and the central role of striatal circuitry for the OCD-like behaviors of *Sapap3* KO mice (8), we next sought to understand how the increased striatal mGluR5 activity of *Sapap3* KO mice (12,13) affects striatal circuit output. Previously, we found that mGluR5 signaling weakens excitatory corticostriatal synaptic strength at striatal projection neurons (SPNs) in the dorsolateral striatum (12,13). Although this finding is ostensibly at odds with the increased striatal firing rates observed in *Sapap3* KO mice in vivo (4), mGluR5 signaling affects numerous cellular properties and cell types within the striatal microcircuit, making it difficult to predict its integrated effect on SPN firing rates. For example, in SPNs, mGluR5 signaling potentiates *N*-methyl-D-aspartate–type glutamate receptor currents (29), disinhibits gamma-aminobutyric acidergic synapses (30), increases intrinsic excitability (31), and mediates corticostriatal synaptic long-term depression (32). Moreover, two key striatal interneuron types that influence SPN activity—fast-spiking and cholinergic interneurons—are also modulated by mGluR5 (33,34).

To elucidate how the various consequences of elevated striatal mGluR5 signaling ultimately integrate within the striatal microcircuit to affect SPN firing, we used an approach we recently established that measures striatal output while preserving the influence of local circuit features (28). With the use of multiphoton laser vector-line scan microscopy of the calcium indicator dye, Fura-2, to visualize APs, we evoked SPN Firing by electrical stimulation of excitatory afferents (28) (Figure 2A–C). The acute slice preparation was used to isolate the striatum from ongoing activity in other brain regions, thereby allowing us to

specifically determine the local striatal contribution of elevated mGluR5 signaling. We further defined effects according to each of the two main classes of striatal projection neurons. The striatonigral or “direct” pathway and the striatopallidal or “indirect” pathway (dSPNs and iSPNs, respectively) can have opposing effects on behavior (35–39), and imbalance of these two basal ganglia pathways has long been hypothesized to underlie movement disorders (40–42) and OCD (43). By taking advantage of the high fidelity of the *Drd1a*-tdTomato reporter to assign SPN types (23), we were able to evaluate activity in both projection pathways simultaneously and with defined spatial relations (Figure 2D, E).

We first examined whether synaptically evoked dSPN and iSPN firing was altered in the dorsolateral striatum of *Sapap3* KO mice. We found that spike probability was significantly increased in both dSPNs ($F_{1,2564} = 110.2$, $p < .0001$) and iSPNs ($F_{1,2052} = 7.6$, $p = .006$; Figure 2F, Supplemental Figure S2A) of *Sapap3* KO mice. In addition, the amplitude of evoked events, an indicator of the number of APs fired per evoked response, was also increased (Figure 2G, Supplemental Figure S2B). However, this effect was only statistically significant in dSPNs ($F_{1,2564} = 112.9$, $p < .0001$ for dSPNs; $F_{1,2052} = 2.4$, $p = .12$ for iSPNs). For both spike probability and event amplitude, we found that the balance of activity between dSPNs and iSPNs in *Sapap3* KO mice was markedly shifted to favor the action-promoting, direct pathway. By comparison, in WT control mice, the balance of activity slightly favors the indirect pathway (Figure 2H, I, Supplemental Figure S3A, B), consistent with a previous report that demonstrated that iSPNs have a higher spontaneous rate of firing in vivo than dSPNs (44).

To determine the contribution of striatal mGluR5 signaling to the circuit disruptions of *Sapap3* KO mice, we treated dorsolateral striatal slices acutely with either MTEP (concentration 20 μmol/L) or vehicle. MTEP significantly reduced spike probability (dSPNs: $F_{1,2780} = 115.2$, $p < .0001$; iSPNs: $F_{1,1948} = 33.1$, $p < .0001$)and event amplitude (dSPNs: $F_{1,2780} = 263.4$, $p < .0001$; iSPNs: $F_{1,1948} = 41.7$, $p < .0001$) in both projection pathways (Figure 3A–D, Supplemental Figure S2C, D) and restored pathway balance (Figure 3E, F). These results show that striatal output is increased and imbalanced toward the direct pathway in *Sapap3* KO mice, and acute MTEP treatment normalizes the circuit abnormalities.

## Constitutive Ligand-Independent Activity Mediates Ongoing mGluR5 Signaling in *Sapap3* KO Mice

Our findings of acute reversal of both the striatal output abnormalities (Figure 2) and OCD-like behaviors (Figure 1) of *Sapap3* KO mice by MTEP indicated a role for ongoing mGluR5 signaling. Ongoing mGluR5 signaling in *Sapap3* KO mice could be driven by increased glutamate-dependent receptor activation and/or by ligand-independent, constitutive signaling that has been described for this receptor (45). Although we previously established that SPNs in *Sapap3* KO mice exhibit increased functional responses to ligand-dependent stimulation relative to WT SPNs (12), we hypothesized that constitutively active receptors might also contribute to elevated mGluR5 signaling in this model. For example, disruption of postsynaptic density scaffold protein interactions, specifically reduced mGluR5 binding to the long isoform of Homer, has been associated with constitutive mGluR5

signaling (45). Because SAPAPs are part of the postsynaptic density scaffold (46), absence of SAPAP3 might functionally uncouple long Homer/mGluR5-dependent signaling and lead to constitutive mGluR5 activity.

To test whether loss of SAPAP3 reduced mGluR5/long Homer interactions, we subjected striatal brain extracts from *Sapap3* KO and WT mice to immunoprecipitation using antibodies that recognize the long Homer isoform. Although no significant differences in total levels of mGluR5 or long Homer were identified in the striatal extracts, the amount of mGluR5 that co-immunoprecipitated with long Homer was significantly reduced in *Sapap3* KO relative to WT striata (Figure 4A – D). These data indicate that SAPAP3 deletion reduces long Homer association with mGluR5, a finding predicted to cause ligand-independent constitutive mGluR5 signaling (45).

To test for constitutive mGluR5 activity, we compared effects of a competitive antagonist [(+)-alpha-methyl-4-car-boxyphenylglycine; MCPG] with those of a NAM (MTEP). We examined drug effects on mEPSCs to minimize activation of presynaptic autoreceptors (group II mGluRs) that are also MCPG targets. In agreement with our previous findings using another mGluR5 NAM (13), acute MTEP treatment increased mEPSC frequency of *Sapap3* KO dSPNs (Figure 4E, F). By contrast, the competitive antagonist MCPG was ineffective (Figure 4G, H). In addition, as expected (13), MTEP did not alter WT responses (Figure 4I, J).

To demonstrate the relation between uncoupling long Homer/mGluR5 scaffolds and SPN activity in *Sapap3* KO mice, we examined the effect of a peptide containing the mGluR5 C-terminal sequence that binds to Homer (mGluR5-CT) (47) on excitatory synaptic transmission in SPNs from *Sapap3* KO and WT mice. We reasoned that if constitutive signaling in *Sapap3* KO mice arose from disrupted mGluR5/ long Homer interactions, then the peptide's effects of dissociating mGluR5 from long Homer might be occluded in *Sapap3* KO mice. As predicted, in WT control mice, the amplitude of evoked EPSCs was significantly reduced in SPNs exposed to mGluR5-CT compared with SPNs exposed to a mutated control peptide ($F_{1,120} = 21.9$, $p < .0001$). However, in *Sapap3* KO mice, this effect was occluded (Figure 4K – M). Notably, KO mice responses were similar to the mGluR5-CT–reduced WT responses. Together, this series of experiments provides biochemical and pharmacologic evidence that disrupted long Homer/mGluR5 scaffolds in *Sapap3* KO mice alter SPN activity through constitutive mGluR5 receptor signaling.

## Acute mGluR5 Potentiation Recapitulates Core Features of OCD-like Behaviors

Although our results thus far indicate the necessity of mGluR5 activity for the OCD-like behavioral and circuit abnormalities in *Sapap3* KO mice, our finding of constitutive mGluR5 signaling further suggests that increased mGluR5 signaling may be an underlying mechanism to drive OCD-like behaviors. To test this idea directly, we pharmacologically augmented endogenous mGluR5 activity in C57BL/6 mice using the highly selective mGluR5 positive allosteric modulator (PAM), VU 0360172 (48).

We found that a single i.p. injection of VU 0360172 caused robust and immediate grooming in C57BL/6 mice that was markedly greater than vehicle control levels ($F_{1,20} = 17.0$, $p = .$

0005; Figure 5B). This drug effect was not present in *Grm5* KO mice (24), confirming mGluR5 target specificity ($F_{1,20}$ = 174.1, $p$ < .0001; Figure 5C). Although C57BL/6 mice treated with PAM exhibited more robust grooming behaviors than mice treated with vehicle, time spent grooming was also significantly increased by vehicle treatment alone. A similar trend was observed in vehicle treatment of WT littermates of *Sapap3* KO mice (which were on a hybrid strain background) (Figure 1B). These findings are consistent with prior observations of grooming behaviors triggered by novelty or stressors and modulated by strain (49). Notably, acute injection-related increases in grooming were absent in C57BL/6 mice that lacked *Grm5* (Figure 5C), indicating a requirement for mGluR5 signaling.

In the OF, VU 0360172 treatment showed a trend to produce the anxiety-like phenotype of reduced center time (Figure 5D, E). However, a role for mGluR5 in this behavior was robustly supported when responses between WT and litter-mate *Grm5* KO mice were compared ($F_{1,16}$ = 48.0, $p$ < .0001; Figure 5F, G). In addition, VU 0360172 had significant effects on other anxiety measures. VU 0360172 decreased the percentage of time spent in the open arms of the EZM ($t_{33}$ = 3.8, $p$ = .0006; Figure 5H) and increased the latency to enter (latency $t_{41}$ = 2.6, $p$ = .013), and it decreased the time spent in the brightly lit chamber of the LDE ($t_{41}$ = 3.3, $p$ = .002; Figure 5J, K). In summary, these experiments show that acute augmentation of endogenously driven mGluR5 activity in normal mice is sufficient to acutely recapitulate the core symptoms of grooming and anxiety-like behaviors that characterize the persistent OCD-like phenotype of the *Sapap3* KO model.

## DISCUSSION

In this study, we have identified excessive mGluR5 signaling as a novel molecular mechanism for OCD-like behaviors. We show that increased and ongoing mGluR5 activity drives OCD-relevant circuit and behavioral phenotypes in mice. Importantly, mGluR5 is a proposed therapeutic target for a number of neurologic and neuropsychiatric disorders (50–53). Thus, a fuller understanding of the effects of mGluR5 signaling on the brain and behavior stands to benefit the successful implementation of this emerging therapy.

Surprisingly, although mGluR5 signaling in the striatum is well known for its role in inducing long-term synaptic plasticity (32), in this study we found that ongoing “real-time” signaling by mGluR5 was responsible for OCD-like behaviors. Behavioral responses occurred within minutes of acute, single treatments with either an mGluR5 NAM to inhibit symptoms in the *Sapap3* KO model or an mGluR5 PAM to elicit symptoms in normal mice. These rapid response rates are in marked contrast to the prolonged treatments periods that are required (days to weeks) to either treat patients and mouse models with selective serotonin reuptake inhibitors (3,8,54), the current clinical treatment mainstay, or induce repetitive grooming activity in mice via optogenetic stimulation of corticostriatal afferents (3). Thus, our observations suggest that mGluR5 signaling is a proximal effector of OCD-like behavior.

In this study, we also reveal that elevated striatal mGluR5 signaling in the *Sapap3* KO model is associated with disruption of mGluR5/Homer-long complexes and constitutive signaling. Disrupted mGluR5/Homer-long interactions are well described in the fragile X mouse model

(55,56), a model that also has increased mGluR5 activity (50), as well as under circumstances with increased expression of short Homer isoforms or mGluR5-CT Homer binding motifs (55,56). Our findings presented here expand our understanding of the specific postsynaptic disruptions that can lead to increased mGluR5 activity.

Increased striatal activity has been associated with OCD behaviors in both clinical populations (5–7) and animal models (3,4). In this study, we found that acute mGluR5 antagonism was sufficient to reduce elevated striatal SPN activity of *Sapap3* KO mice both in vivo when delivered systemically and ex vivo when applied locally to acute slices. In addition to increasing SPN firing, we further found that activity between dSPNs and iSPNs was imbalanced in *Sapap3* KO mice.

An overarching model for the contribution of the basal ganglia circuit to motor behavior emphasizes the mutually antagonistic roles of the direct and indirect pathways in promoting and inhibiting movement, respectively (40–42). Consistent with this, optogenetic manipulations of SPNs provide proof of principle that movement can be grossly influenced accordingly (36). In the present study, by imaging SPNs in both pathways simultaneously, we were able to directly examine balance and provide the first experimental evidence that OCD-like behaviors are associated with basal ganglia pathway imbalance (Figure 3, Supplemental Figure S3). Independent of the pathway imbalance, the observed change in gain (Figure 2C, D) is also predicted to have behaviorally significant effects. At least computationally, increased corticostriatal gain is predicted to lower the decision time threshold for motor responses and to come at a cost of reduced reward optimization (57). In addition, we recently found that increased striatal gain correlates with habitual behavior (28). Thus, although speculative, such effects could contribute to the increased, and ultimately deleterious, expression of routines in OCD. Of note, although our study focuses on dorsolateral striatal circuit abnormalities to reveal the effects of mGluR5 signaling, our findings do not rule out behavioral contributions from other striatal subregions, including ventral striatum or extrastriatal brain regions.

Interestingly, although an increase in SPN AP firing from elevated mGluR5 signaling is opposite to the prediction that would be derived based on the known effects of mGluR5 for weakening corticostriatal excitatory synaptic strength (12,13), our observation is concordant with recent findings in early striatal development, whereby increased evoked SPN firing rates and weaker corticostriatal synaptic strength coexist (58). In *Sapap3* KO mice, mGluR5-mediated increases in SPN activity could arise through a number of local circuit mechanisms, including, but not limited to, increased SPN intrinsic excitability (31) and endocannabinoid-mediated suppression of inhibitory synaptic tone (30,59). Importantly, given how any single isolated feature may fail to accurately predict the net circuit output, we show here the utility of an integrated measure of striatal output in that it accurately reflects the in vivo state (4) and can be used to identify therapies that act locally to normalize circuit output (Figure 3).

Clinically, obsessive-compulsive (O-C) behaviors occur in a wide variety of contexts. Furthermore, genetic studies and clinical observations indicate that OCD itself is a heterogeneous disorder (60). In this study, we provide proof of principle that increased

mGluR5 signaling may be a convergent end point driving O-C behaviors. We show that increasing mGluR5 signaling through two distinct mechanisms causes OCD-like behaviors; the first by loss of *Sapap3* in KO mice and the second by pharmacologic mGluR5 augmentation in normal mice. Of course, although we refer to the constellation of behaviors in the *Sapap3* KO model as "OCD-like," future studies in humans are necessary to determine whether related striatal mGluR5 pathophysiology will be identified in OCD per se or other behavioral disorders. Therefore, an important translational issue is to identify whether and which clinical populations have increased striatal mGluR5 activity. Fortunately, suitable mGluR5 radioligands have recently become available to aid in this endeavor (61–63).

In summary, the results of this study provide preclinical support for overactive mGluR5 signaling as a tractable mechanism-based target to develop new treatments for O-C behaviors. The alacrity of the mGluR5 NAM effects on behavior shown here are in marked contrast to the current clinical treatment mainstay and suggest that targeting mGluR5 or its proximate downstream signaling events may enable faster symptom relief and/or improved efficacy. Moreover, a fuller appreciation of the behavioral consequences of mGluR5 signaling informs the development and monitoring of drugs targeting mGluR5, both PAMs and NAMs, as they are optimized for use in patients in a variety of clinical settings.

## Supplementary Material

Refer to Web version on PubMed Central for supplementary material.

## Acknowledgments

This work was supported by National Institute of Neurological Disorders and Stroke Grant No. NS064577 (to NC), American Recovery & Reinvestment Act of 2009 supplement to Grant No. NS064577 (to NC) and Grant No. NS045711 (to KMH); Brain and Behavioral Research Foundation Young Investigator Award (to KKA); National Institute of Neurological Disorders and Stroke Grant No. T32NS051156 (to KKA); and FRAXA Research Foundation (to WG).

We thank members of the Calakos laboratory for helpful discussions and technical support; A. Contractor for providing *Grm5* null mice, S. Tracy, J. Cruger, and K. Tsukayama for mouse genotyping and husbandry; M. Shipman for technical assistance; T. Rhodes and the Duke University Neurobehavioral Core Facility staff for assistance with behavioral experiments; K. Tsukayama and T. Stanek for assistance with figure graphics; S. Mague for technical assistance with the in vivo recordings; and J. Ting for suggestions for slice buffers. We thank H. Marie, S. Soderling, C. Kuo, and S. Lisberger for critical reading of the manuscript.

## References

1. McGuire JF, Lewin AB, Horng B, Murphy TK, Storch EA. The nature, assessment, and treatment of obsessive-compulsive disorder. Postgrad Med. 2012; 124:152–165. [PubMed: 22314125]
2. Zohar AH. The epidemiology of obsessive-compulsive disorder in children and adolescents. Child Adolesc Psychiatr Clin N Am. 1999; 8:445–460. [PubMed: 10442225]
3. Ahmari SE, Spellman T, Douglass NL, Kheirbek MA, Simpson HB, Deisseroth K, et al. Repeated cortico-striatal stimulation generates persistent OCD-like behavior. Science. 2013; 340:1234–1239. [PubMed: 23744948]
4. Burguiere E, Monteiro P, Feng G, Graybiel AM. Optogenetic stimulation of lateral orbitofronto-striatal pathway suppresses compulsive behaviors. Science. 2013; 340:1243–1246. [PubMed: 23744950]

5. Guehl D, Benazzouz A, Aouizerate B, Cuny E, Rotge JY, Rougier A, et al. Neuronal correlates of obsessions in the caudate nucleus. Biol Psychiatry. 2008; 63:557–562. [PubMed: 17945196]
6. Hansen ES, Hasselbalch S, Law I, Bolwig TG. The caudate nucleus in obsessive-compulsive disorder. Reduced metabolism following treatment with paroxetine: a PET study. Int J Neuropsychopharmacol. 2002; 5:1–10. [PubMed: 12057027]
7. Maltby N, Tolin DF, Worhunsky P, O'Keefe TM, Kiehl KA. Dysfunctional action monitoring hyperactivates frontal-striatal circuits in obsessive-compulsive disorder: an event-related fMRI study. Neuroimage. 2005; 24:495–503. [PubMed: 15627591]
8. Welch JM, Lu J, Rodriguiz RM, Trotta NC, Peca J, Ding JD, et al. Cortico-striatal synaptic defects and OCD-like behaviours in Sapap3-mutant mice. Nature. 2007; 448:894–900. [PubMed: 17713528]
9. Bienvenu OJ, Wang Y, Shugart YY, Welch JM, Grados MA, Fyer AJ, et al. Sapap3 and pathological grooming in humans: Results from the OCD collaborative genetics study. Am J Med Genet B Neuropsychiatr Genet. 2009; 150B:710–720. [PubMed: 19051237]
10. Stewart SE, Yu D, Scharf JM, Neale BM, Fagerness JA, Mathews CA, et al. Genome-wide association study of obsessive-compulsive disorder. Mol Psychiatry. 2013; 18:788–798. [PubMed: 22889921]
11. Zuchner S, Wendland JR, Ashley-Koch AE, Collins AL, Tran-Viet KN, Quinn K, et al. Multiple rare SAPAP3 missense variants in trichotillomania and OCD. Mol Psychiatry. 2009; 14:6–9. [PubMed: 19096451]
12. Chen M, Wan Y, Ade K, Ting J, Feng G, Calakos N. Sapap3 deletion anomalously activates short-term endocannabinoid-mediated synaptic plasticity. J Neurosci. 2011; 31:9563–9573. [PubMed: 21715621]
13. Wan Y, Feng G, Calakos N. Sapap3 deletion causes mGluR5-dependent silencing of AMPAR synapses. J Neurosci. 2011; 31:16685–16691. [PubMed: 22090495]
14. Mehta MV, Gandal MJ, Siegel SJ. mGluR5-antagonist mediated reversal of elevated stereotyped, repetitive behaviors in the VPA model of autism. PLoS One. 2011; 6:e26077. [PubMed: 22016815]
15. Silverman JL, Tolu SS, Barkan CL, Crawley JN. Repetitive self-grooming behavior in the BTBR mouse model of autism is blocked by the mGluR5 antagonist MPEP. Neuropsychopharmacology. 2010; 35:976–989. [PubMed: 20032969]
16. Aguilar-Valles A, Matta-Camacho E, Khoutorsky A, Gkogkas C, Nader K, Lacaille JC, et al. Inhibition of group I metabotropic glutamate receptors reverses autistic-like phenotypes caused by deficiency of the translation repressor eIF4E binding protein 2. J Neurosci. 2015; 35:11125–11132. [PubMed: 26245973]
17. Egashira N, Okuno R, Harada S, Matsushita M, Mishima K, Iwasaki K, et al. Effects of glutamate-related drugs on marble-burying behavior in mice: implications for obsessive-compulsive disorder. Eur J Pharmacol. 2008; 586:164–170. [PubMed: 18423440]
18. Kalinichev M, Le Poul E, Bolea C, Girard F, Campo B, Fonsi M, et al. Characterization of the novel positive allosteric modulator of the metabotropic glutamate receptor 4 ADX88178 in rodent models of neuropsychiatric disorders. J Pharmacol Exp Ther. 2014; 350:495–505. [PubMed: 24947466]
19. Egashira N, Abe M, Shirakawa A, Niki T, Mishima K, Iwasaki K, et al. Effects of mood stabilizers on marble-burying behavior in mice: Involvement of GABAergic system. Psychopharmacology. 2013; 226:295–305. [PubMed: 23086022]
20. Kalariya M, Prajapati R, Parmar SK, Sheth N. Effect of hydroalcoholic extract of leaves of Colocasia esculenta on marble-burying behavior in mice: Implications for obsessive-compulsive disorder. Pharm Biol. 2015; 53:1239–1242. [PubMed: 25885941]
21. Kantak PA, Bobrow DN, Nyby JG. Obsessive-compulsive-like behaviors in house mice are attenuated by a probiotic (Lactobacillus rhamnosus GG). Behavioural Pharmacology. 2014; 25:71–79. [PubMed: 24257436]
22. Honda S, Kawaura K, Soeda F, Shirasaki T, Takahama K. The potent inhibitory effect of tipepidine on marble-burying behavior in mice. Behav Brain Res. 2011; 216:308–312. [PubMed: 20713091]

23. Ade KK, Wan Y, Chen M, Gloss B, Calakos N. An improved BAC transgenic fluorescent reporter line for sensitive and specific identification of striatonigral medium spiny neurons. Front Syst Neurosci. 2011; 5:32. [PubMed: 21713123]
24. Xu J, Zhu Y, Contractor A, Heinemann SF. mGluR5 has a critical role in inhibitory learning. J Neurosci. 2009; 29:3676–3684. [PubMed: 19321764]
25. Rodgers RJ, Shepherd JK. Influence of prior maze experience on behaviour and response to diazepam in the elevated plus-maze and light/dark tests of anxiety in mice. Psychopharmacology (Berl). 1993; 113:237–242. [PubMed: 7855188]
26. Shepherd JK, Grewal SS, Fletcher A, Bill DJ, Dourish CT. Behavioural and pharmacological characterisation of the elevated "zero-maze" as an animal model of anxiety. Psychopharmacology (Berl). 1994; 116:56–64. [PubMed: 7862931]
27. Dzirasa K, Fuentes R, Kumar S, Potes JM, Nicolelis MA. Chronic in vivo multi-circuit neurophysiological recordings in mice. J Neurosci Methods. 2011; 195:36–46. [PubMed: 21115042]
28. O'Hare JK, Ade KK, Sukharnikova T, Van Hooser SD, Palmeri ML, Yin HH, et al. Pathway-specific striatal substrates for habitual behavior. Neuron. 2016; 89:472–479. [PubMed: 26804995]
29. Pisani A, Gubellini P, Bonsi P, Conquet F, Picconi B, Centonze D, et al. Metabotropic glutamate receptor 5 mediates the potentiation of N-methyl-D-aspartate responses in medium spiny striatal neurons. Neuroscience. 2001; 106:579–587. [PubMed: 11591458]
30. Dvorzhak A, Semtner M, Faber DS, Grantyn R. Tonic mGluR5/ CB1-dependent suppression of inhibition as a pathophysiological hallmark in the striatum of mice carrying a mutant form of huntingtin. J Physiol. 2013; 591:1145–1166. [PubMed: 23230231]
31. D'Ascenzo M, Podda MV, Fellin T, Azzena GB, Haydon P, Grassi C. Activation of mGluR5 induces spike afterdepolarization and enhanced excitability in medium spiny neurons of the nucleus accumbens by modulating persistent Na+ currents. J Physiol. 2009; 587:3233–3250. [PubMed: 19433572]
32. Sung KW, Choi S, Lovinger DM. Activation of group I mGluRs is necessary for induction of long-term depression at striatal synapses. J Neurophysiol. 2001; 86:2405–2412. [PubMed: 11698530]
33. Bonsi P, Cuomo D, De Persis C, Centonze D, Bernardi G, Calabresi P, et al. Modulatory action of metabotropic glutamate receptor (mGluR) 5 on mGluR1 function in striatal cholinergic interneurons. Neuropharmacology. 2005; 49(suppl 1):104–113. [PubMed: 16005029]
34. Bonsi P, Sciamanna G, Mitrano DA, Cuomo D, Bernardi G, Platania P, et al. Functional and ultrastructural analysis of group I mGluR in striatal fast-spiking interneurons. Eur J Neurosci. 2007; 25:1319–1331. [PubMed: 17425558]
35. Ferguson SM, Phillips PE, Roth BL, Wess J, Neumaier JF. Direct-pathway striatal neurons regulate the retention of decision-making strategies. J Neurosc. 2013; 33:11668–11676.
36. Kravitz AV, Freeze BS, Parker PR, Kay K, Thwin MT, Deisseroth K, et al. Regulation of parkinsonian motor behaviours by opto-genetic control of basal ganglia circuitry. Nature. 2010; 466:622–626. [PubMed: 20613723]
37. Kravitz AV, Tye LD, Kreitzer AC. Distinct roles for direct and indirect pathway striatal neurons in reinforcement. Nat Neurosci. 2012; 15:816–818. [PubMed: 22544310]
38. Lobo MK, Covington HE III, Chaudhury D, Friedman AK, Sun H, Damez-Werno D, et al. Cell type-specific loss of BDNF signaling mimics optogenetic control of cocaine reward. Science. 2010; 330:385–390. [PubMed: 20947769]
39. Tai LH, Lee AM, Benavidez N, Bonci A, Wilbrecht L. Transient stimulation of distinct subpopulations of striatal neurons mimics changes in action value. Nat Neurosci. 2012; 15:1281–1289. [PubMed: 22902719]
40. Albin RL, Young AB, Penney JB. The functional anatomy of basal ganglia disorders. Trends Neurosci. 1989; 12:366–375. [PubMed: 2479133]
41. DeLong MR. Primate models of movement disorders of basal ganglia origin. Trends Neurosci. 1990; 13:281–285. [PubMed: 1695404]
42. Nelson AB, Kreitzer AC. Reassessing models of basal ganglia function and dysfunction. Annu Rev Neurosci. 2014; 37:117–135. [PubMed: 25032493]

43. Baxter LR Jr, Saxena S, Brody AL, Ackermann RF, Colgan M, Schwartz JM, et al. Brain mediation of obsessive-compulsive disorder symptoms: Evidence from functional brain imaging studies in the human and nonhuman primate. Semin Clin Neuropsychiatry. 1996; 1:32–47. [PubMed: 10229782]
44. Mallet N, Ballion B, Le Moine C, Gonon F. Cortical inputs and GABA interneurons imbalance projection neurons in the striatum of parkinsonian rats. J Neurosci. 2006; 26:3875–3884. [PubMed: 16597742]
45. Ango F, Prezeau L, Muller T, Tu JC, Xiao B, Worley PF, et al. Agonist-independent activation of metabotropic glutamate receptors by the intracellular protein Homer. Nature. 2001; 411:962–965. [PubMed: 11418862]
46. Welch JM, Wang D, Feng G. Differential mRNA expression and protein localization of the SAP90/PSD-95-associated proteins (SAPAPs) in the nervous system of the mouse. J Comp Neurol. 2004; 472:24–39. [PubMed: 15024750]
47. Mao L, Yang L, Tang Q, Samdani S, Zhang G, Wang JQ. The scaffold protein Homer1b/c links metabotropic glutamate receptor 5 to extracellular signal-regulated protein kinase cascades in neurons. J Neurosci. 2005; 25:2741–2752. [PubMed: 15758184]
48. Rodriguez AL, Grier MD, Jones CK, Herman EJ, Kane AS, Smith RL, et al. Discovery of novel allosteric modulators of metabotropic glutamate receptor subtype 5 reveals chemical and functional diversity and in vivo activity in rat behavioral models of anxiolytic and antipsychotic activity. Mol Pharmacol. 2010; 78:1105–1123. [PubMed: 20923853]
49. Kalueff AV, Tuohimaa P. Mouse grooming microstructure is a reliable anxiety marker bidirectionally sensitive to GABAergic drugs. Eur J Pharmacol. 2005; 508:147–153. [PubMed: 15680265]
50. Dolen G, Bear MF. Role for metabotropic glutamate receptor 5 (mGluR5) in the pathogenesis of fragile X syndrome. J Physiol. 2008; 586:1503–1508. [PubMed: 18202092]
51. Doria JG, de Souza JM, Andrade JN, Rodrigues HA, Guimaraes IM, Carvalho TG, et al. The mGluR5 positive allosteric modulator, CDPPB, ameliorates pathology and phenotypic signs of a mouse model of Huntington's disease. Neurobiol Dis. 2015; 73:163–173. [PubMed: 25160573]
52. Matosin N, Newell KA. Metabotropic glutamate receptor 5 in the pathology and treatment of schizophrenia. Neurosci Biobehav Rev. 2013; 37:256–268. [PubMed: 23253944]
53. Picconi B, Calabresi P. Targeting metabotropic glutamate receptors as a new strategy against levodopa-induced dyskinesia in Parkinson's disease? Mov Disord. 2014; 29:715–719. [PubMed: 24591264]
54. Fineberg NA, Gale TM. Evidence-based pharmacotherapy of obsessive-compulsive disorder. Int J Neuropsychopharmacol. 2005; 8:107–129. [PubMed: 15450126]
55. Giuffrida R, Musumeci S, D'Antoni S, Bonaccorso CM, Giuffrida-Stella AM, Oostra BA, et al. A reduced number of metabotropic glutamate subtype 5 receptors are associated with constitutive homer proteins in a mouse model of fragile X syndrome. J Neurosci. 2005; 25:8908–8916. [PubMed: 16192381]
56. Ronesi JA, Collins KA, Hays SA, Tsai NP, Guo W, Birnbaum SG, et al. Disrupted Homer scaffolds mediate abnormal mGluR5 function in a mouse model of fragile X syndrome. Nat Neurosci. 2005; 15:431–440. S431.
57. Lo CC, Wang XJ. Cortico-basal ganglia circuit mechanism for a decision threshold in reaction time tasks. Nature Neuroscience. 2006; 9:956–963. [PubMed: 16767089]
58. Peixoto RT, Wang W, Croney DM, Kozorovitskiy Y, Sabatini BL. Early hyperactivity and precocious maturation of corticostriatal circuits in Shank3B mice. Nat Neurosci. 2016; 19:716–724. [PubMed: 26928064]
59. Centonze D, Rossi S, Prosperetti C, Gasperi V, De Chiara V, Bari M, et al. Endocannabinoids limit metabotropic glutamate 5 receptor-mediated synaptic inhibition of striatal principal neurons. Mol Cell Neurosci. 2007; 35:302–310. [PubMed: 17434747]
60. Pauls DL, Abramovitch A, Rauch SL, Geller DA. Obsessive-compulsive disorder: an integrative genetic and neurobiological perspective. Nat Rev Neurosci. 2014; 15:410–424. [PubMed: 24840803]

61. Akkus F, Terbeck S, Ametamey SM, Rufer M, Treyer V, Burger C, et al. Metabotropic glutamate receptor 5 binding in patients with obsessive-compulsive disorder. Int J Neuropsychopharmacol. 2014; 17:1915–1922. [PubMed: 24833114]

62. Wong DF, Waterhouse R, Kuwabara H, Kim J, Brasic JR, Chamroonrat W, et al. 18F–FPEB, a PET radiopharmaceutical for quantifying metabotropic glutamate 5 receptors: a first-in-human study of radiochemical safety, biokinetics, and radiation dosimetry. J Nucl Med. 2013; 54:388–396. [PubMed: 23404089]

63. Rook JM, Tantawy MN, Ansari MS, Felts AS, Stauffer SR, Emmitte KA, et al. Relationship between in vivo receptor occupancy and efficacy of metabotropic glutamate receptor subtype 5 allosteric modulators with different in vitro binding profiles. Neuropsychopharmacology. 2015; 40:755–765. [PubMed: 25241804]

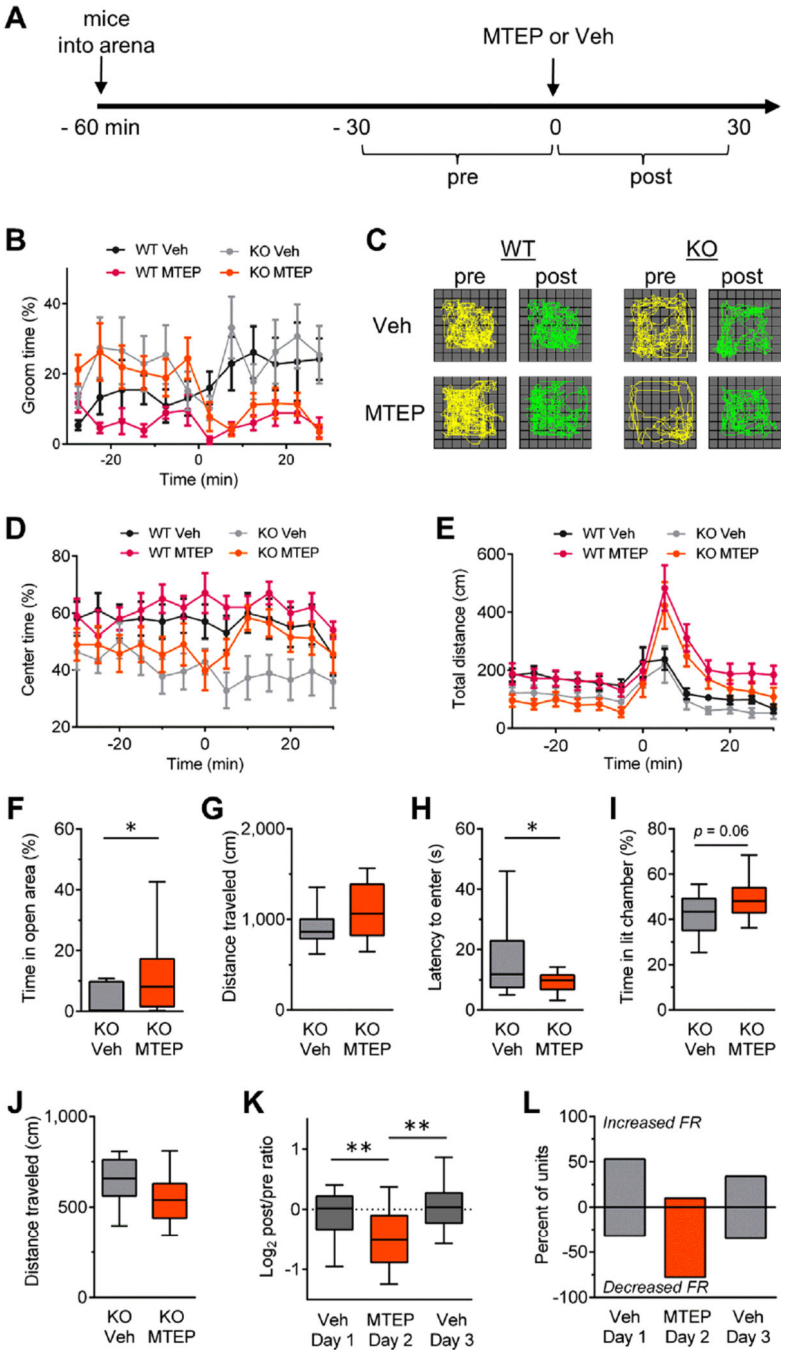


**Figure 1.**

Type 5 metabotropic glutamate receptor antagonism reduces obsessive-compulsive disorder–like behaviors in *Sapap3* knockout (KO) mice. **(A)** Experimental design for evaluating the effects of MTEP (20 mg/kg, i.p.) in wild-type (WT) and *Sapap3* KO mice in the open field (OF) (**B–E**). Injections of either MTEP or vehicle control (Veh) were given at time = 0 minutes. Drug modulation of behavior was evaluated for each genotype by comparing the 30-minute interval before (pre) and after (post) injection. WT vehicle $n = 9$, WT MTEP $n = 14$, KO vehicle $n = 12$, KO MTEP $n = 12$. **(B)** Grooming activity time course shows MTEP

reduces basal grooming levels in *Sapap3* KO mice but not WT mice. **(C)** Locomotor trajectories of representative WT and *Sapap3* KO mice in the OF during 10-minute periods before and after injections of vehicle or MTEP. Time courses showing **(D)** center time and **(E)** total distance traveled in the OF. Time course data are presented as means ± SEMs. **(F–J)** Boxplots showing anxiolytic effects of MTEP in *Sapap3* KO mice. For the elevated zero maze, **(F)** percentage of time spent in the open area and **(G)** locomotion ($n$ = 17–18 per group). For the light-dark emergence, **(H)** latency to enter the brightly lit chamber, **(I)** percentage of time spent in the brightly lit chamber, and **(J)** locomotion ($n$ = 15–17 per group). Boxplots showing **(K)** normalized change in striatal firing rate (FR) relative to preinjection period for striatal units recorded in vivo and **(L)** summary of units showing a change in firing rate during the postinjection period relative to the preinjection baseline with magnitudes >10%. Veh day 1, $n$ = 201 units/4 mice; MTEP day 2, $n$ = 231 units/4 mice; Veh day 3, $n$ = 207 units/4 mice. Boxplots present median, upper, and lower quartiles, and upper and lower 90%. *$p$ < .05, **$p$ < .01. i.p., intraperitoneal.

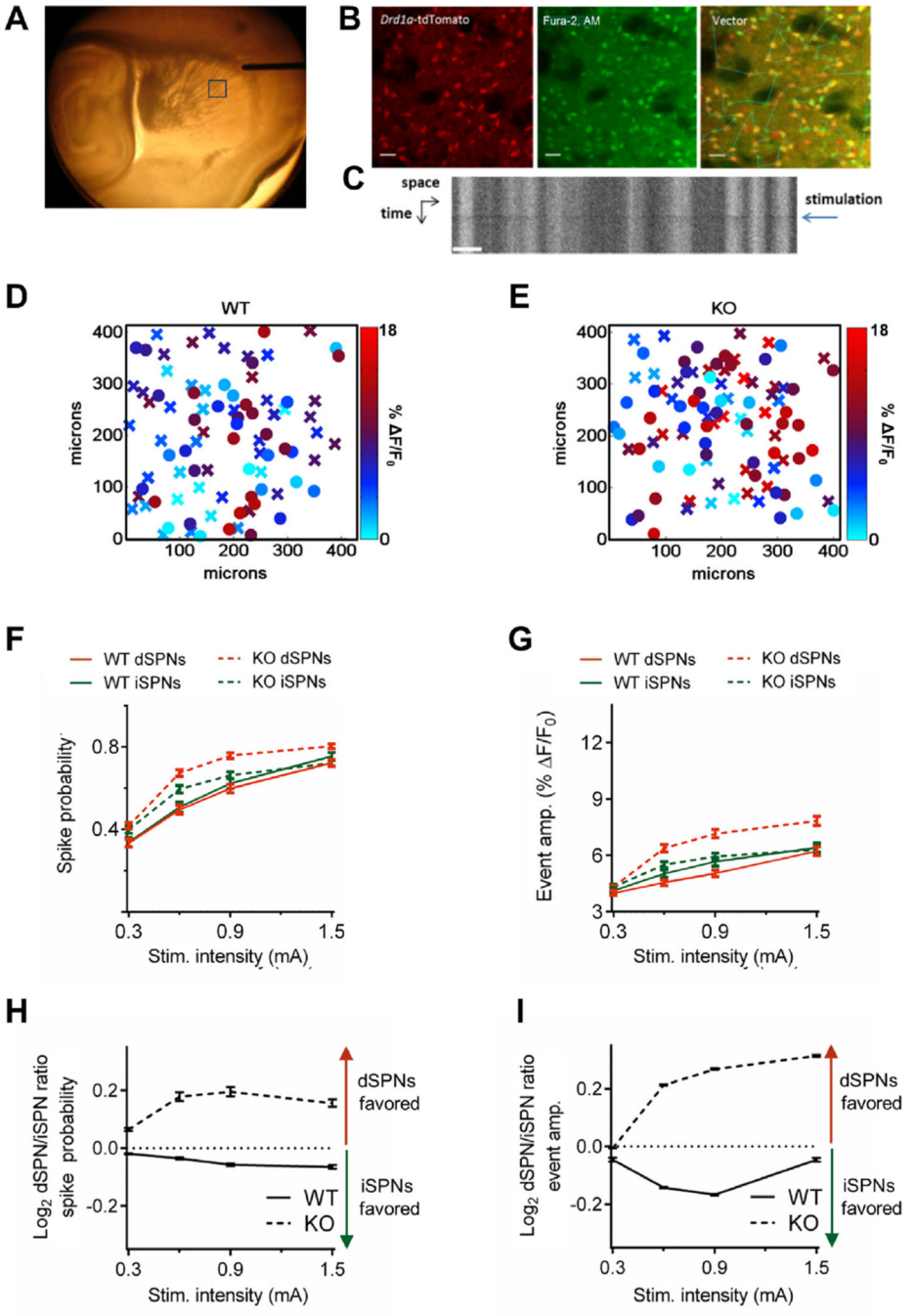


**Figure 2.**

Striatal projection neuron (SPN) output is increased and imbalanced in *Sapap3* knockout (KO) mice. **(A)** Representative image showing extracellular stimulating electrode placement in acute brain slice. Fields were imaged 600–650 μm from the tip of the electrode along the path of incoming cortical afferents. The box indicates the location of a typical field of view. **(B)** Representative raster scans showing fluorescence of *Drd1a*-tdTomato transgene (left), Fura-2 (middle), and overlay with vector path used for line-scan imaging (right). Scale bar = 25 μm. **(C)** Kymograph showing that Fura-2 fluorescence decreases at the time of

extracellular stimulation (Stim.) (blue arrow). Scale bar = 15 μm. Heat maps of direct SPN (dSPN; "X") and indirect SPN (iSPN; "O") event amplitudes (amp.) in the X–Y space showing representative responses to stimulation of cortical afferents (0.6 mA) in brain slices from **(D)** wild-type (WT) and **(E)** *Sapap3* KO mice demonstrate that the genotype effects on firing properties were broadly distributed in space. Summaries of **(F)** spike probability and **(G)** event amplitude demonstrate that SPN-evoked firing rates are increased in *Sapap3* KO mice relative to their WT littermates. Summaries of dSPN/iSPN ratios for **(H)** spike probability and **(I)** event amplitude demonstrate that the relative balance of striatal output is shifted in favor of the direct pathway in *Sapap3* KO mice relative to their WT littermates. WT = 262 dSPNs/197 iSPNs, 6 slices, 3 mice; *Sapap3* KO = 381 dSPNs/318 iSPNs, 9 slices, 6 mice. Data are presented as means ± SEMs.

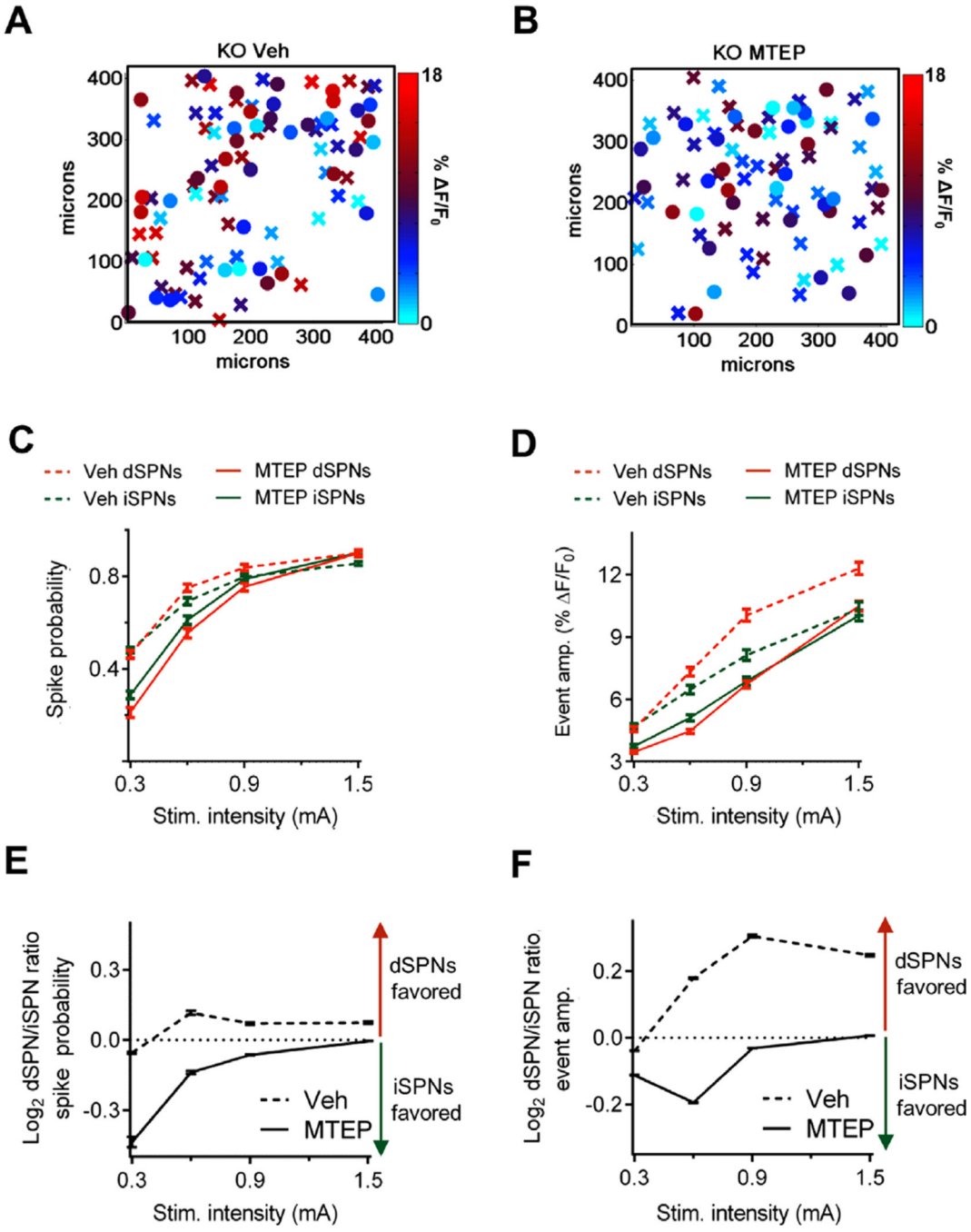


**Figure 3.**

Striatal type 5 metabotropic glutamate receptor signaling increases and unbalances of striatal project neuron (SPN) output in *Sapap3* knockout (KO) mice. Heat maps of direct SPN (dSPN; "X") and indirect SPN (iSPN; "O") event amplitudes (amp.) in the X–Y space showing representative responses to stimulation (Stim.) of cortical afferents (0.6 mA) in brain slices from *Sapap3* KO mice treated with either **(A)** vehicle (Veh) or **(B)** MTEP. Summaries of **(C)** spike probability and **(D)** event amplitude demonstrate that MTEP decreases the SPN-evoked firing rate in *Sapap3* KO mice. Summaries of dSPN/iSPN ratios

for **(E)** spike probability and **(F)** event amplitude demonstrate that MTEP reverses the striatal pathway imbalance in *Sapap3* KO mice. Veh: *n*= 313 dSPNs/205 iSPNs, 6 slices, 3 mice; MTEP: *n*= 384 dSPNs/284 iSPNs, 8 slices, 4 mice. Data are presented as means ± SEMs.

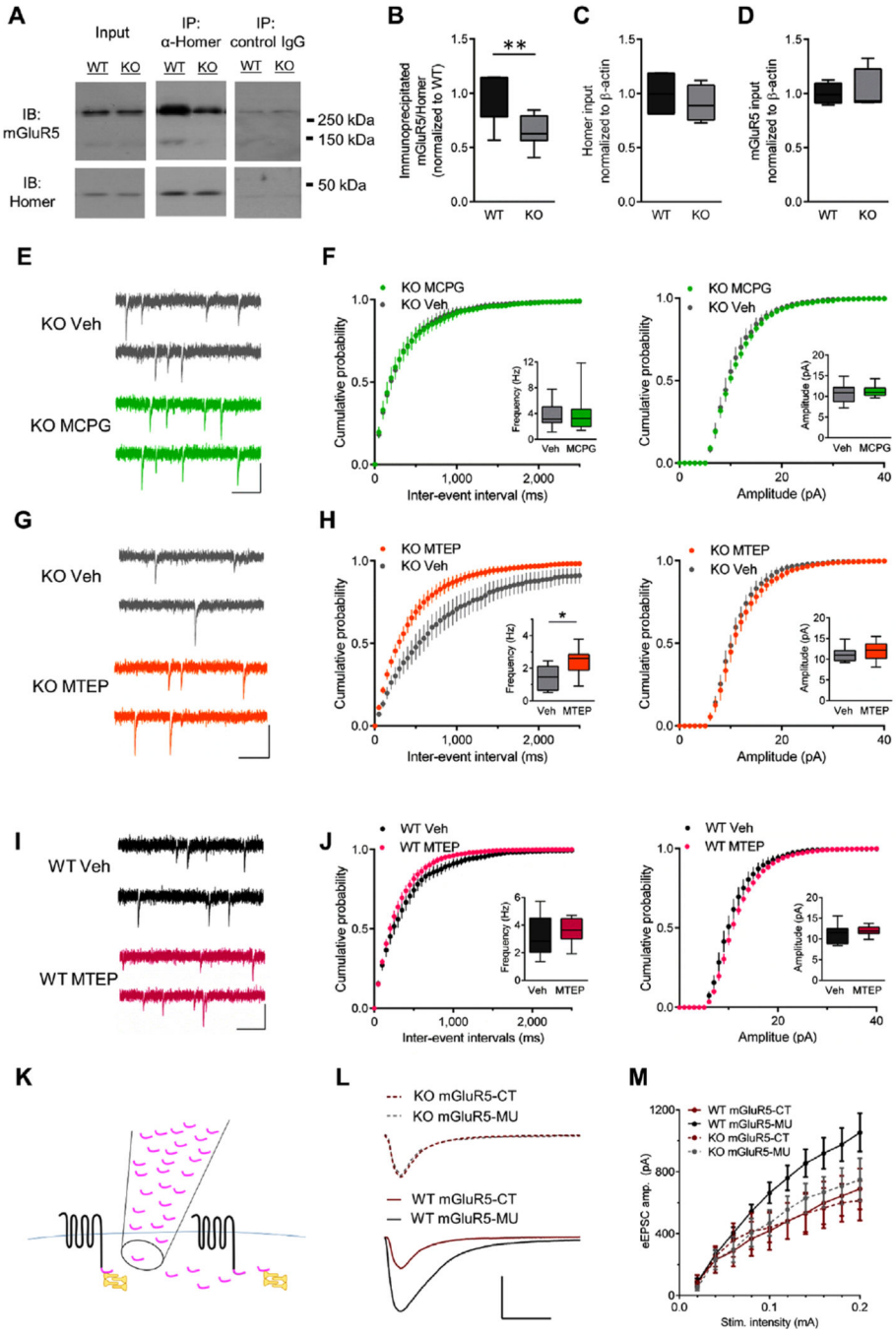


**Figure 4.**

Constitutive signaling contributes to ongoing type 5 metabotropic glutamate receptor (mGluR5) activity in *Sapap3* knockout (KO) mice. **(A)** Representative Western immunoblots (IBs) from a littermate pair showing that *Sapap3* deletion reduces co-immunoprecipitation (IP) of mGluR5 (monomers approximately 130 kDa, dimers approximately 260 kDa) with the long Homer isoform. Boxplots showing **(B)** significantly less mGluR5 co-immunoprecipitated with long Homer in KO relative to wild-type (WT) striatal extracts; however, input levels of **(C)** long Homer and **(D)** mGluR5 were not significantly different

between WT and *Sapap3* KO striatal extracts ($n$ = 7–8 per group). **(E)** Representative traces and **(F)** summary data showing that MCPG (500 μmol/L) does not affect miniature excitatory postsynaptic current (mEPSC) frequency (left) or amplitude (right) in direct striatal projection neurons (dSPNs) in *Sapap3* KO mice ($n$= 11 for both groups). **(G)** Representative traces and **(H)** summary data showing that MTEP significantly increases mEPSC frequency (left) but not amplitude (amp.) (right) in dSPNs in *Sapap3* KO mice ($n$ = 9 for both groups). **(I)** Representative traces and **(J)** summary data showing that MTEP (concentration 20 μmol/L) does not affect mEPSC frequency (left) or amplitude (right) in dSPNs in WT mice [vehicle (Veh), $n$= 7; MTEP, $n$= 9]. **(E, G**, and **I)** Scale bars = 25 pA, 200 ms. Boxplots present median, upper and lower quartiles, and upper and lower 90%. *$p$ < .05, **$p$ < .01. **(K)** Schematic showing that peptide corresponding to C-terminus of mGluR5 (mGluR5-CT; pink) competitively interferes with mGluR5 (black) and Homer (yellow) interactions. **(L)** Representative responses to 0.2-mA stimulation and **(M)** summary data demonstrate that mGluR5-CT reduces evoked EPSC amplitude in WT but not KO dSPNs (WT mGluR5-CT, $n$ = 8; WT mGluR5-MU, $n$ = 6; KO mGluR5-CT, $n$ = 6; KO mGluR5-MU, $n$ = 5). Scale bar = 500 pA, 20 ms. MU, mutated; Stim., stimulation.

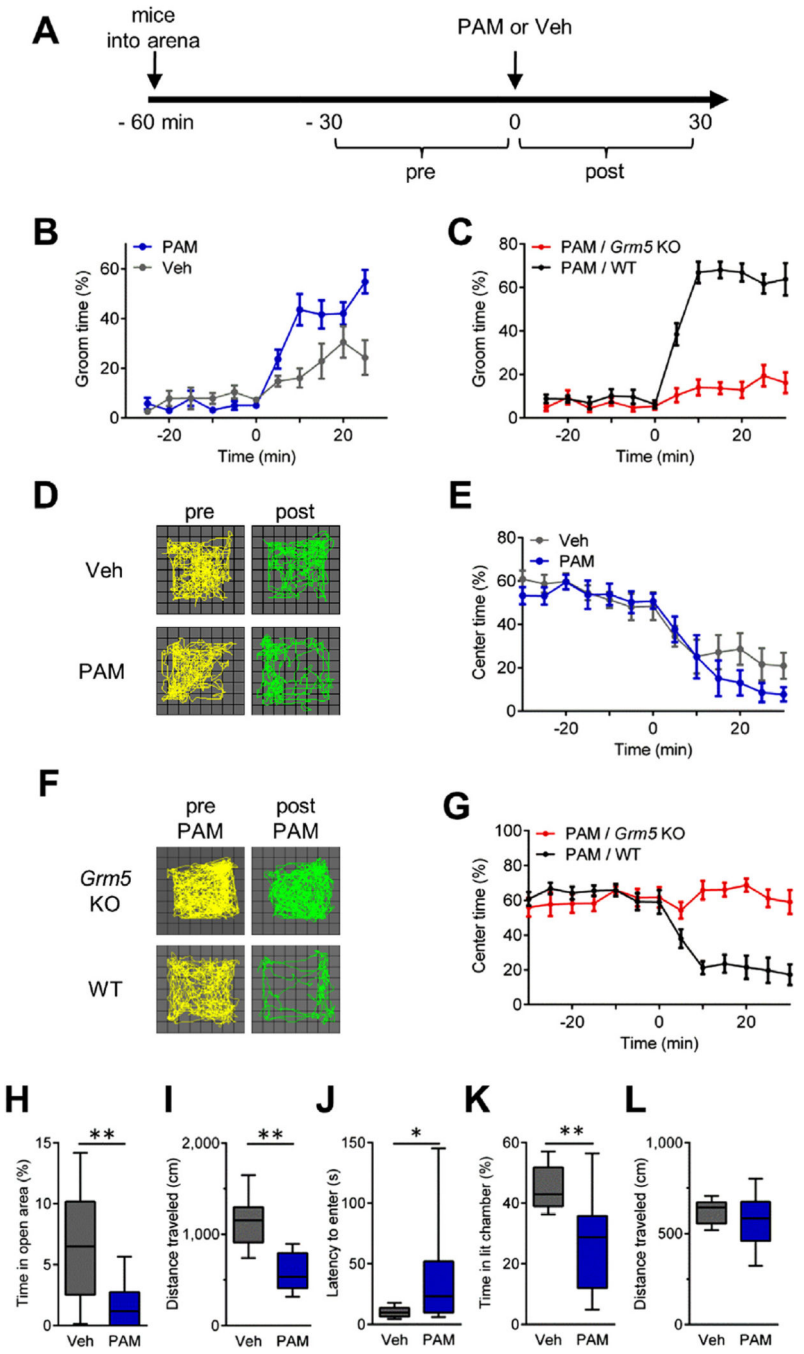


**Figure 5.**

Acute type 5 metabotropic glutamate receptor (mGluR5) potentiation induces obsessive-compulsive disorder–like behaviors in C57BL/6 mice. **(A)** Experimental design for evaluating the effects of the mGluR5 positive allosteric modulator (PAM), VU 0360172 (20 mg/kg, i.p.), or vehicle (Veh) on C57BL/6 mice **(B, D**, and **E)** and VU 0360172 (20 mg/kg, i.p.) on *Grm5* knockout (KO) and wild-type (WT) littermates **(C, F, and G)** in the open field (OF). Injections were given at time = 0 minutes. Modulation of behavior by PAM was evaluated by comparing the 30-minute postinjection periods between groups. Grooming

activity time course data show **(B)** PAM significantly increases basal grooming levels in C57BL/6 mice ($n = 11$ for both conditions) and **(C)** that the grooming effects of PAM depend on mGluR5 signaling (*Grm5* KO, $n = 7$; WT, $n = 11$). **(D)** Locomotor trajectories of representative C57BL/6 mice in the OF during 10-minute periods before and after injections of Veh (top) or PAM (bottom). **(E)** Time course showing the percentage of time C57BL/6 mice spent in the center of the OF arena. **(F)** Locomotor trajectories of a representative *Grm5* KO mouse (top) and WT mouse (bottom) in the OF during 10-minute periods before and after injections of PAM. **(G)** Time course showing the percentage of time WT and *Grm5* KO mice spent in the center of the OF arena. Time course data are presented as means ± SEMs. **(H–L)**, Boxplots showing anxiolytic effects of PAM. For the elevated zero maze, **(H)** time spent in the open area and **(I)** locomotion ($n = 17–18$ per group). For the light-dark emergence, **(J)** latency to enter the brightly lit chamber, **(K)** time spent in the brightly lit chamber, and **(L)** locomotion ($n = 21–22$ per group). Boxplots present median, upper and lower quartiles, and upper and lower 90%. *$p < .05$, **$p < .01$. i.p., intraperitoneal.